1 Variation in drug penetration does not account for the natural resistance 2 of Mycobacterium abscessus biofilms to antibiotic 3 Winifred C. Akwani<sup>1,4,5\*</sup>, Paulina Rakowska<sup>3</sup>, Ian Gilmore<sup>4</sup>, Mark Chambers<sup>1,2</sup>, Greg 4 M<sup>c</sup>Mahon<sup>4</sup> and Suzie Hingley-Wilson<sup>1</sup>. 5 6 7 **Affiliation** 8 1. Department of Microbial Sciences, School of Biosciences and Medicine, Faculty of 9 Health and Medical Sciences, University of Surrey, Guildford, GU2 7XH, UK 2. Department of Comparative Biomedical Sciences, School of Veterinary Medicine, 10 Faculty of Health and Medical Sciences, University of Surrey, Guildford GU2 7AL, UK 11 3. National Biofilms Innovation Centre (NBIC), University of Southampton, Southampton, 12 SO17 1BJ, UK 13 4. National Physical Laboratory, National Centre of Excellence in Mass Spectrometry 14 Imaging (NiCE- MSI), Teddington, Middlesex TW11 0LW, UK 15 5. Current Affiliation: London Centre for Nanotechnology, University College London, 16 London, WC1H 0AH, UK 17 \*Corresponding authors 18 Winifred C. Akwani 19 London Centre for Nanotechnology, University College London, London, WC1H 0AH, UK 20 w.akwani@ucl.ac.uk 21 22 Keywords 23 Mycobacterium abscessus, Biofilms, Antibiotic resistance, Scanning Electron Microscopy 24 (SEM), Nanoscale secondary ion mass spectrometry (NanoSIMS) 25 26 27 28 29

**Abstract** 

30

33

34

35

36

41

45

54

55

56

57

59

60

61

62

31 Mycobacterium abscessus, an inherently drug-resistant, opportunistic, nontuberculous

32 mycobacterium (NTM) predominantly causes pulmonary infections in immunocompromised

patients, notably those with cystic fibrosis. M. abscessus subspecies display distinct colony

morphologies (rough and smooth), with the prevalent view that M. abscessus (smooth) is a

persistent, biofilm-forming phenotype, whilst *M. abscessus* (rough) is unable to form biofilms.

Biofilm formation contributes to persistent infections and exhibits increased antibiotic

37 resistance.

38 We used the chemical mapping technique, nanoscale secondary ion spectrometry

39 (NanoSIMS), to investigate if variations in the biofilm morphology and antibiotic penetration

40 account for the antibiotic susceptibility amongst *M. abscessus* subspecies, contributing to

increased antimicrobial resistance (AMR) and potentially explaining the protracted treatment

42 duration.

The susceptibility to bedaquiline (BDQ) of *M. abscessus* grown as planktonic bacilli and

44 biofilms was measured. The minimum biofilm eradication concentration (MBEC) of BDQ was

8-16 times higher (2-4µg/ml) compared with the minimum inhibitory concentration (MIC)

46 (0.25μg/ml), indicating reduced efficacy against biofilms.

47 Correlative imaging with electron microscopy revealed that *M. abscessus* (irrespective of the

48 colony morphotype) formed biofilms and that BDQ treatment influenced biofilm morphology.

49 We determined that *M. abscessus* morphotypes exhibit differential uptake of the antibiotic

50 BDQ in biofilms. *M. abscessus* subsp. *abscessus* (smooth) biofilms exhibited the least uptake

of BDQ, whereas M. abscessus subsp. bolletii biofilms showed the greatest antibiotic

52 penetration.

NanoSIMS analysis revealed no correlation between antibiotic penetration and drug efficacy

within the biofilm. This challenges the previous assumption linking biofilm architecture to drug

efficacy. Investigating other biofilm characteristics like antibiotic persistence could lead to

enhanced treatment approaches.

# Significance Statement

58 Mycobacterium abscessus is an increasingly prevalent pathogen, most often causing lung

infections in immunocompromised individuals. Their distinct morphotypes and biofilm-forming

capabilities contribute to persistent infections, rendering them challenging to treat with

increased antibiotic resistance. This research demonstrates that the antibiotic, bedaquiline

exhibits significantly reduced efficacy against M. abscessus growing as a biofilm compared to

- 63 planktonic growth, but that the efficiency of antibiotic penetration was not the main explanation
- 64 for the different susceptibilities of MABC biofilms to treatment.

# **Main Text**

### Introduction

Mycobacterium abscessus complex (MABC) is a group of rapidly growing, nontuberculous mycobacteria (NTMs) frequently associated with pulmonary infections, but also skin and soft tissue infections (1, 2). MABC comprises of three subspecies: *M. abscessus* subsp. abscessus subsp. bolletii and *M. abscessus* subsp. massiliense (3), which exhibit two colony morphotypes; rough and smooth, based on the absence or presence of the cell wall glycopeptidolipids (GPLs) (4). These species can form biofilms contributing to localised infections, especially in the lungs (4–6). Biofilms are defined as a community of aggregated bacteria enveloped in an extracellular matrix (ECM) (7–9). This growth mechanism renders them notoriously tolerant to antibiotics, contributing to the treatment recalcitrance of *M. abscessus*. This is often thought to be due poor penetration of antibiotic into the biofilm leading to subinhibitory concentrations reaching the bacteria.

Establishing standardized antibiotic susceptibility testing methods with good *in vitro-in vivo* correlation is a significant challenge in managing MABC infections as susceptibility testing outcomes do not align with treatment success against these infections (10, 11). In addition, the conventional minimum inhibitory concentration (MIC) testing, used to measure antibiotic efficacy against bacteria undergoing planktonic growth, does not align with the concentrations required to combat biofilms (12). Macrolides are crucial for treating MABC infections, but their effectiveness is limited due to macrolide resistant MABC strains (13–15). Alternative agents like Bedaquiline (BDQ) are being explored to address these challenges. BDQ inhibits the proton pump of ATP synthase, an enzyme that is required for cellular respiration (16, 17). This bromine-containing diarylquinoline shows promise, with low MIC values against MABC isolates offering a potential treatment option for these challenging infections (18–20)

In biofilms, the ECM provides stability to the biofilm structure but may also act as a protective layer and diffusion barrier inhibiting antibiotic penetration to access single cells. Advanced imaging techniques can play a valuable role in understanding the interaction and penetration of antibiotics into bacterial biofilms. For example, scanning electron microscopy (SEM) provides high-resolution imaging of the biofilm architecture at the level of individual bacterial cells (21) Studies using SEM have shown that biofilm cells exposed to antibiotics undergo morphological changes (22, 23).

Nanoscale secondary ion mass spectrometry (NanoSIMS) offers the ability to simultaneously detect up to seven isotopic masses at subcellular spatial resolution, enabling the mapping of labelled molecule distributions within cells. NanoSIMS is capable of distinguishing specific subcellular structures and has been combined with electron microscopy techniques to characterise cellular ultrastructure (24). This correlative approach has been used to study the activity of pyrazinamide (PZA) and BDQ on *Mycobacterium tuberculosis* within human macrophages, revealing how these drugs accumulate within bacterial cells and impact their efficacy (25) and to track the distribution of BDQ within individual cells in murine infected lungs revealing its localisation within intracellular bacteria and specific cell types (26)However, to date there have not been any studies investigating antibiotic penetration into NTM planktonic cells or biofilms using NanoSIMS.

This study aims to evaluate the efficacy of BDQ against MABC growing planktonically or as biofilms and assess its bactericidal action using a variety of readouts: minimal bactericidal concentration (MBC); minimal biofilm eradication concentration (MBEC); minimal biofilm inhibitory concentration (MBIC) and biofilm bactericidal concentration (BBC). These data are correlated with the results of the SEM and NanoSIMS imaging on the impact of BDQ on biofilm structure and its ability to penetrate biofilms and reach individual bacterial cells.

#### Results

96

97

98

99 100

101

102

103

104

105

106

107

108

109110

111

112

113

114

120

# MIC of BDQ against MABC (planktonic bacteria)

- Drug susceptibility testing was performed using broth microdilution to determine the minimum
- inhibitory concentration (MIC) of BDQ for the MABC as planktonic bacterial cells. The species
- were exposed to a range of antibiotic concentrations, BDQ (0.0039-2 µg/ml) for an incubation
- period of 3 days. The MIC of BDQ for MABC was 0.25 µg/ml [Figure 1(A)], consistent with
- other reports (27, 28).

# **Determining BDQ susceptibility against MABC biofilms**

- 121 The efficacy BDQ to inhibit and/or eradicate MABC biofilms was tested. The mycobacterial
- species were exposed to 2-fold increasing antibiotic concentrations for 24 hours to determine
- the biofilm susceptibility endpoint parameters i.e. MBC, MBIC, MBEC and BBC, using the MIC
- value (0.25 μg/ml) for the planktonic cell as a starting concentration. The concentration of BDQ
- ranged between 0.25-32 µg/ml in the MBC, MBIC, MBEC and BBC assays.
- Table 1 shows an overview of the MBC, MBIC, MBEC and BBC of BDQ determined for MABC
- 127 biofilms.

128 The MBC, MBEC, MBIC and BBC concentrations for MABC biofilms were significantly higher

in comparison with the planktonic cells. The MBC for MABC was 4 µg/ml, except for

M. abscessus subsp. massiliense, which was 2 μg/ml. MBIC values for M. abscessus subsp.

abscessus biofilms (rough and smooth morphotypes) were consistent at 4 µg/ml, while

M. abscessus subsp. massiliense biofilms had the lowest value (1 μg/ml). Conversely,

M. abscessus subsp. bolletii biofilms required a higher inhibitory concentration (16 μg/ml). The

MBEC for MABC (4 µg/ml) indicated BDQ had an inhibitory effect on biofilms [Figure 1(B)].

The BBC concentration (>32 µg/ml) across all M. abscessus subspecies biofilms revealed

BDQ lacked a bactericidal effect (Supplementary Figures).

# Morphology and structure of MABC biofilms exposed to BDQ imaged by SEM

138 MABC biofilms were grown on sterile silicon chips and incubated for 7 days at 37°C. They

were exposed to BDQ (4 µg/ml, based on MBEC results) for 24 hours before freeze-drying

and SEM visualisation. SEM was used to assess the effect of BDQ on the morphology of the

141 freeze-dried *M. abscessus* (subspecies) biofilms.

129

130

131

132

133

134

135

136

137

139

140

143

144

145

146

147

148

149

150

152

153

154

155

156

157

158

160

162

In untreated *M. abscessus* (rough) biofilms, SEM images revealed compactly embedded rod-

shaped bacilli within a dense matrix [red arrows in Figure 2(Aii)]. However, with BDQ addition,

SEM images showed less dense, porous M. abscessus (rough) biofilms compared to

untreated samples [Figure 2(Aiv-vi)]. BDQ caused the breakdown of the dense matrix and

altered the morphology of the bacilli from rod-shaped to round-shaped [indicated by a red

circle in Figure 2(Avi)]. Similarly, *M. abscessus* (smooth) biofilms displayed intermingled bacilli

within a highly dense, porous matrix [yellow arrow in Figure 2(Bi)]. The addition of BDQ to

M. abscessus (smooth) biofilms showed a breakdown of the ECM and the release of individual

bacilli [Figure 2(Biv-vi)]. BDQ also disrupted the cell membrane of M. abscessus (smooth),

resulting in altered membrane structure [indicated by yellow arrows in Figure 2(Bvi)].

Untreated M. bolletii biofilms exhibited a network-like structure of bacilli within the matrix

[Figure 2(Ci-iii)]. However, in treated *M. bolletii* biofilms, the network structure was disrupted

with thread-like connections between bacilli and an increased number of elongated individual

bacilli [green arrows in Figure 2(Cv)]. Like M. abscessus (rough), M. massiliense biofilms

showed compactly embedded bacilli within a dense matrix [Figure 2(Di-iii)]. BDQ addition

caused the ECM breakdown and the release of bacilli embedded within the matrix. In addition,

BDQ caused destruction of the cell membrane in *M. massiliense*, resulting in alterations to its

structure [indicated by blue arrows in Figure 2(Dvi)].

### Distribution of Br at a single-cell level within MABC biofilms

161 The intensity of the total Br ion signal (a distinct marker for BDQ) was measured using

NanoSIMS to determine the localisation of BDQ within the biofilms by summing the <sup>79</sup>Br and

<sup>81</sup>Br<sup>-</sup> ion images. The <sup>12</sup>C<sub>2</sub><sup>-</sup> and <sup>12</sup>C<sup>14</sup>N<sup>-</sup> signals provided information on the structure of the cells within the MABC biofilms. Treated *M. abscessus* biofilms showed the Br<sup>-</sup> ion signal within the cellular components, indicating the uptake of the lipophilic BDQ by cells of the biofilms, especially in the cell wall/matrix [Figure 3(A-D)].

# Quantitative analysis of the uptake of BDQ into MABC biofilms

Quantitative analysis was carried out using the ratio distribution Br<sup>-</sup>/<sup>12</sup>C<sup>14</sup>N<sup>-</sup> and Br<sup>-</sup>/<sup>12</sup>C<sub>2</sub><sup>-</sup> to compare antibiotic penetration (based on the same BDQ concentration used) in the treated and untreated MABC biofilms. The quantitative analysis showed that there was significantly higher bromine uptake into the cell wall/matrix of *M. abscessus* subsp. *bolletii* biofilms compared with the other subspecies [Figure 4].

### **Discussion**

163 164

165

166

167

168

169170

171

172

173

174

175

176

177178

179

180 181

182

183

184 185

186

187

188

189 190

191

192 193

194

195

196

Bedaquiline has been considered as a prospective antibiotic for the treatment of *M. abscessus* infections. Based on *in vitro* studies, BDQ has shown promising antibiotic efficacy against NTM species (29) and shown to be a good growth inhibitor at low doses against *M. abscessus* subspecies (19, 27, 30). However, it has been reported that BDQ does not have bactericidal activity against *M. abscessus* in vivo (19, 31, 32) which would be in-keeping with the findings in this study that *M. abscessus* subspecies exhibited reduced efficacy to BDQ as biofilm.

Antibiotic resistance is a hallmark of biofilm formation. Our results highlight that *M. abscessus* can form biofilms irrespective of morphotype. Based on the MIC of BDQ obtained for planktonic growth in this study, the MBEC assay was used to determine different biofilm susceptibility endpoint parameters (MBC, MBIC, MBEC and BBC) for subspecies of M. abscessus. These biofilm susceptibility endpoint parameters have been used as a guide for biofilm related infections. However, there are huge discrepancies between their definitions and parameters, therefore there is a need to have standardized definitions for these biofilm endpoints similar to the MIC (33). Based on previous studies (34-38) and for the context of this study, the MBEC was used as the biofilm susceptibility endpoint parameter to make comparison with the MIC. Our results showed that M. abscessus (subspecies) biofilms were inhibited at higher concentrations of BDQ compared with planktonic growth. In addition, BDQ had a bacteriostatic effect against the biofilms (2-4µg/ml) but needed a much higher concentration to have a bactericidal effect on the biofilms (≥32µg/ml). These findings suggest that while BDQ is considered a potential agent for M. abscessus infections due to its low MIC, it is essential to recognise the complexity introduced by biofilms given their genetic and phenotypic differences. Biofilms are much harder to eradicate compared with planktonic bacteria(39, 40).

M. abscessus subspecies exhibit either a rough or smooth morphotype based on the presence or absence of GPLs on the cell wall (41). Previous studies suggested that only the smooth morphotypes can form extensive biofilms whilst, the rough morphotypes produce either no or little biofilm but can still cause persistent infections (42–44). We studied the morphological heterogeneity of the MABC. SEM showed that both rough and smooth morphotypes were able to form extensive biofilms, contrary to prior findings. Consistent with other studies, M. abscessus (rough) also formed pellicles with a cording formation(34). It is believed that the MmpL protein is involved in the GPL biosynthetic pathway of the cell envelope, and that a mutation of mmpL4a gene causes a deficiency in GPL production and/or transport in the rough morphotype and the capacity to produce cords in vitro (45). The cording formation has been associated with increased pathogenicity and drug resistance (46). Studies have shown that cord-forming isolates such as M. abscessus (rough) are denser and contain a greater number of cells per unit compared with smooth isolates (47), which could reduce antibiotic penetration within the rough morphotype biofilm.

As the unique structural features of biofilms pose a barrier to antibiotic penetration contributing significantly to the emergence of functional antibiotic resistance, we used NanoSIMS imaging to examine the effects of BDQ on these biofilms. Cording formation of *M. abscessus* (rough) is thought to contribute to persistent lung infection and the recalcitrance of antibiotic treatment. Whilst this was consistent with high MBEC and BBC values observed for *M. abscessus* (rough), NanoSIMS analysis expressed as the Br<sup>-</sup>/CN<sup>-</sup> ratio, did not indicate reduced uptake of BDQ into *M. abscessus* (rough) biofilms compared with the other *M. abscessus* subspecies.

The efficacy of antibiotic penetration into biofilms is not solely influenced by the cellular organisation or formation of the biofilm, but also by its cellular components and extracellular matrix (ECM) (48). The ECM contains lipids (GPLs, mycolic acids), polysaccharides, proteins and eDNA (49, 50). Generally, the rough morphotype has a low GPL expression, whereas the presence of the GPL in the smooth isolates has been linked with increased hydrophobicity and biofilm formation (51, 52). Based on the observation of the biofilm structure it can be deduced that *M. abscessus* subsp. *bolletii* likely has a smooth morphotype like *M. abscessus* subsp. *abscessus* (smooth) that expresses the GPL on its cell wall. NanoSIMS analysis showed an increased uptake of BDQ into *M. abscessus* subsp. *bolletii* biofilms (based on the Br/CN<sup>-</sup> ratio values) compared with the other *M. abscessus* subspecies. This is consistent with the observation that the network structure was disrupted in treated *M. bolletii* biofilms, and that the expression of GPL in *M. abscessus* subsp. *bolletii* may have caused the attachment of the lipophilic BDQ to the lipid-rich cell wall. There is very limited information regarding *M. bolletii* strains, specifically in relation to the rough and the smooth morphotypes and/or biofilm formation, despite these strains being associated with pulmonary infections (53–

55). Studies suggest that GPL affects the mechanical properties of *M. abscessus* biofilms, whereby the smooth morphotype exhibited increased pliability compared with the rough morphotype (56). This characteristic could be a contributing factor in the increased uptake of BDQ into *M. bolletti* biofilms. However, this was not followed by increased efficacy of the drug; indeed, *M. bolletti* biofilms exhibited MBEC and BBC values no different to the other subspecies. Furthermore, as we found *M. abscessus* subsp. *abscessus* (smooth) biofilms exhibited least uptake of BDQ, there is a need to further explore the relationship between the structural properties (cords, aggregates) and the chemical composition of the biofilms (including the GPLs, mycolic acids) with antibiotic penetration.

Beyond the primary biofilm resistance mechanism of antibiotic penetration, another contributing factor may be the reduced uptake of antibiotics by oxygen-deprived bacteria within the biofilm. The biofilm architecture can create an oxygen and nutrient gradient. As a result, the outer layers of the biofilms are usually aerobic and metabolically active, whilst the inner layers become anaerobic and nutrient deficient. Most antibiotics are most effective against metabolically active bacteria, so the reduced growth rate on the inner layers of the biofilms could contribute to antibiotic resistance (42, 44, 46). SEM micrographs suggested that the presence of ECM hindered antibiotic penetration of BDQ to effective concentrations in the deeper biofilm layers. As a result, the outer layers of the biofilms exhibited morphological changes and in some of the mycobacterial species ECM degradation, while the deeper layers retained their structural integrity, showing little or no response to the antibiotic treatment.

Biofilm development can be a significant barrier in effective treatment of chronic NTM infections. This is also coupled with *M. abscessus* being intrinsically resistant and/or acquiring resistance to the currently available antibiotics. In this case, *M. abscessus* biofilms limited antibiotic penetration due to their colony morphotypes, biofilm architecture and the cellular composition of the biofilms. In addition, the slower growth rate, hydrophobic nature and/or the metabolic status of the mycobacteria within the biofilms (44, 57, 58), all likely contribute to increased antibiotic resistance. Due to the difficulties in the treatment of biofilm related *M. abscessus* infections, there is a need to know how to incorporate BDQ into these treatment regimens and to maximise its effect. It has been reported that BDQ was more effective in synergy with other antibiotics against disseminated NTM infection in patients co-infected with HIV (59). Further studies are needed to use combinational treatment therapy that include BDQ against *M. abscessus* biofilms and to determine their effects.

In conclusion, the combination of SEM and NanoSIMS imaging techniques allowed for the visualisation of the spatial arrangement of the biofilms, morphological effects of the antibiotic applied to the biofilms and tracking of antibiotic penetration at the single-cell level. These

findings suggest that both the morphology and structure of the MABC biofilms and possibly the composition of the biofilm limited the efficacy of the antibiotics, but that antibiotic penetration alone could not account for the resistance of biofilm to treatment. These results point to the need for a deeper understanding of how the biofilm contributes to functional antibiotic resistance and that better therapeutic strategies need to do more than merely increase antibiotic penetration into biofilms.

### **Materials and Methods**

### Bacterial strains, media, and growth conditions

M. abscessus subsp. abscessus (M. abscessus), M. abscessus subsp. bolletii (M. bolletii), and M. abscessus subsp. massiliense (M. massiliense) clinical isolates were a kind gift from the National Mycobacterium Reference Laboratory, Borstel, Germany. Liquid cultures of mycobacterial species were grown in Middlebrook 7H9 supplemented with 10% Albumin Dextrose Catalase (ADC) (Sigma-Aldrich) for MABC, 0.2% glycerol and 0.05% Tween 80 (Sigma-Aldrich) incubated at 37°C. Overnight cultures contained glass beads to mechanically prevent the clumping of mycobacterial isolates.

### Determination of Minimum inhibitory concentration (MIC) of planktonic MABC

Bedaquiline (BDQ) was purchased from Combi-Blocks (San Diego, USA) and was dissolved in dimethyl sulfoxide (DMSO) at 1mg/ml concentration and stored at -20°C. The minimum inhibition concentration (MIC) assay was performed using broth microdilution as outlined by the Clinical and Laboratory Standard Institute (CLSI) (CLSI, 2011) to determine the lowest antibiotic concentration that inhibited the growth of planktonic cells. Cation-adjusted Mueller-Hinton broth (CAMHB) with 5% OADC was used for the MIC assay of the MABC. The concentrations of BDQ ranged from 2 to 0.0039 μg/ml by serial dilutions in a 96-well microtiter plate. Bacterial cultures were adjusted to approximately 1x10<sup>7</sup> CFU/ml for inoculation. A volume of 50 μl of the diluted inoculum was added to each of well and the final volume in each well was 100 μl. In the experiment, the negative control consisted of just media or antibiotic, whilst the positive control consisted of bacteria alone. The plates were sealed and incubated at 37°C for 3 days. Following incubation, the minimum inhibitory concentration (MIC) was determined by measuring the optical density (OD<sub>600nm</sub>) using a plate reader. The MIC is defined as the minimum antibiotic concentration to inhibit planktonic growth.

### **Biofilm antimicrobial susceptibility of MABC**

Biofilm antimicrobial susceptibility testing was performed using methods previously described (34–38) to determine the minimum biofilm eradication concentration (MBEC). The MBEC biofilm inoculator (Innovotech Inc., Edmonton, Canada) consists of a plastic lid with 96 pegs

and a corresponding base. Bacterial cultures were adjusted to approximately 1x10<sup>6</sup> CFU/ml using Sauton's minimal media and 150µl was dispensed into each well of the MBEC inoculator. Biofilms were formed on the pegs after 3-5 days incubation for 37°C. The mature biofilms (peg lids) were transferred into a new 96 well plate containing serially diluted BDQ from the stock solutions (1mg/ml), which were incubated for 24hrs at 37°C. Following the antimicrobial challenge, the peg lid was rinsed twice in PBS and exposed biofilms were disrupted into recovery media (7H9-ADC- Tween 80- glycerol) by sonication for 10 mins. Negative controls contained just media/antibiotics and positive controls contained bacterial biofilms alone.

# Determination of the minimum bactericidal concentration (MBC) and minimum biofilm

# 311 inhibitory concentration (MBIC)

- To determine the minimum bactericidal concentration (MBC) against *M. abscessus* (subspecies) biofilms, 20 µl of broth suspension from each challenge plate well was combined with 180 µl of fresh CAMH with 5% OADC in a new 96-well plate, sealed, and incubated at 37°C for 3 days. The MBC, defined as the lowest antibiotic concentration that inhibited growth of dispersed cells from the biofilm compared with the growth control. This was determined by measuring optical density at OD<sub>600nm</sub> using a plate reader.
- Concurrently, in the challenge plate, biofilms released planktonic cells into antibioticcontaining broth during the challenge incubation period. Subsequently, a new non-pegged lid was placed on the 96-well challenge plate base and incubated at 37°C for 3 days. Following incubation, the minimum biofilm inhibitory concentration (MBIC) of BDQ was determined by reading the optical density of the challenge plate at OD<sub>600nm</sub>, where MBIC is the minimum antibiotic concentration inhibiting the growth of dispersed cells from the biofilm.

# Determination of minimum biofilm eradication concentration (MBEC) and bactericidal biofilm concentration (BBC)

Following the challenge plate, the MBEC peg lid was transferred to a plate containing 200  $\mu$ l of neutralizer recovery media (CAMH with 5% OADC), then sonicated to dislodge biofilms from the pegs. Planktonic cells in the recovery media were serially diluted ( $10^{0}$ - $10^{7}$ ) in PBS with Tween 80, and 20  $\mu$ l of each diluted sample were spotted on Middlebrook 7H11 agar. The plates were then incubated for 3-5 days at 37°C. To determine the BBC, the colonies were counted and expressed as Log<sub>10</sub> CFU/ml. BBC is defined as the lowest antibiotic concentration killing 99.9% of biofilm – embedded bacteria compared to the growth control.

After the Log<sub>10</sub> biofilm reduction, the volume of the neutralizer recovery media used for serial dilution was replaced with fresh media. The plate was covered with a new sterile non-pegged lid and incubated at 37°C for 3 days. After incubation, the MBEC was determined by measuring

the optical density at OD<sub>600nm</sub>. MBEC is defined as the minimum antimicrobial concentration

that eliminates the biofilm.

### Statistical analysis

336

337

338

345346

348

349350

351

352

353354

355

356

358

359

360

361

363

364

365

367

- 339 All experimental assays were carried out at least three times and their averages were
- 340 determined where necessary. All data acquired in the study were statistically analysed using
- 341 GraphPad Prism version 9.1.1 for Windows, GraphPad Software, Boston, Massachusetts
- 342 USA, www.graphpad.com, to determine the *p* values and establish any correlation between
- untreated and treated MABC biofilms using two-way ANOVA. If within the data sets, the p-
- value is less than 0.05 it was considered statistically significant.

# Sample preparation of MABC biofilms for Scanning Electron microscopy (SEM) and

# Nanoscale secondary ion mass spectrometry (NanoSIMS)

347 *M. abscessus* and subspecies were grown in Sauton's minimal media on sterile silicon wafer

chips (Agar Scientific Ltd., Stansted, UK) within a 6-well plate. The plates were incubated at

37°C without shaking to allow biofilm formation. After the incubation period, BDQ was added

to the mycobacterial biofilm samples based on the concentration obtained from the MBEC

assay. PBS was added as a negative control to the samples. Both samples were incubated at

37°C for 24 hours. After the incubation with and without antibiotics, the mycobacterial biofilm

samples were rinsed with ultrapure water. The samples were placed in a -80°C freezer

overnight and then placed into the freeze dryer (Modulyo, Edwards, UK) at -40°C with a

pressure of 60-80 mbar, overnight. Once the samples were dried, they were either sputter

gold-coated at a thickness 9 nm using a Quorum (Laughton, East Sussex, UK) sputter coater

for SEM or left to air dry for NanoSIMS analysis.

### Scanning Electron Microscopy (SEM)

The cell morphology of the freeze-dried mycobacterial biofilms on silicon chips before and

after the addition of the antibiotic (24 hours) treatment was assessed by SEM. Conductive

adhesive carbon tabs were added to aluminium specimen mount stubs (12.5 mm) (Agar

362 Scientific) and the silicon chips with the biofilms were carefully attached onto the top. The

biofilm samples were viewed with a field emission SEM (JSM-7100F, JEOL BV, Zaventem,

Belgium) using the secondary electron detector with an accelerating voltage of 5kV and probe

current of 6 pA. SEM experiments were carried out in triplicate for samples with/without

366 antibiotics.

# Nanoscale Secondary Ion Mass Spectrometry (NanoSIMS)

Nanoscale Secondary Ion Mass Spectrometry (NanoSIMS) (CAMECA, Gennevilliers France) was used to map and detect ions that are specific to the antibiotic ( $Br^- - BDQ$ )] within the mycobacterial biofilms. In addition, NanoSIMS was used in detecting the elements that can be found within the mycobacterial species ( $^{12}C^{14}N^-, ^{12}C_2^-$ ).

The sample was bombarded by a primary ion beam from a Cs $^+$  source at a potential of +8 kV. The sample is biased at – 8 kV to extract negative secondary ions. Thus, the net impact kinetic energy of the ion beam is 16 keV. The resulting secondary ions ( $^{12}C^{14}N^-$ , $^{12}C_2^-$ , $^{79}Br^-$ ,  $^{81}Br^-$ ) are steered through an electrostatic sector where they are filtered for energy and then to a magnetic sector mass analyser and are separated by their mass-to charge ratio. The positions of a set of electron multiplier detectors, with single ion sensitivity are adjusted so that one detector records the signal from one selected secondary ion mass. Signal is acquired at each pixel while the primary Cs beam is scanned across the sample surface, forming images. NanoSIMS has a high spatial resolution of <50 nm which allows for the identification of isotopic composition within individual bacteria samples at subcellular resolution. Images were acquired at either 128 x 128 or 256 x 256 pixels with primary beam currents ranging from 0.5 – 1.0 pA.

# **NanoSIMS Imaging analysis**

The ion signals obtained from the images were quantified using ImageJ with the OpenMIMS plugin (github.com/BWHCNI/OpenMIMS, Harvard Center for NanoImaging). Image processing included image alignment, image summing, selecting the region of interest (ROIs) using the CN and/or C<sub>2</sub> images, extracting ion count intensities from the ROIs, and statistical analysis (60) and adding the scale bars. For the visualization of the uptake of BDQ in the bacteria, a ratio metric image was produced with Br<sup>-</sup>/<sup>12</sup>C<sup>14</sup>N<sup>-</sup> x 10000.

**Acknowledgements** This work was supported by the Engineering and Physical Sciences Research Council (EP/S51391X/1) and the UK Department of Science, Innovation and Technology and the National Measurement System program. We would like to thank Dr Florian Maurer from Diagnostic Mycobacteriology, National Reference Center for Mycobacteria for providing all of the Nontuberculous mycobacteria (NTMs) strains used. We thank David Jones, Sarah Barnett-Tucker and Andreas Lakovidis from MicroStructural Studies Unit (MSSU), the electron microscopy facility of the University of Surrey for all the support provided on the SEM. We thank Dr. G. Greenidge and Dr. G. Trindade for reviewing the manuscript. **Author Contributions** All authors contributed to the conception and the design of this study. W.A. and G.M. contributed to the acquisition and analysis of data. All authors contributed to the writing of the manuscript. **Competing Interest Statement** The authors declare no conflict of interest.

# References

- 429 1. M. Brodlie, *et al.*, Bile acid aspiration in people with cystic fibrosis before and after lung transplantation. *European Respiratory Journal* **46**, 1820–1823 (2015).
- 431 2. K. P. Fennelly, *et al.*, Biofilm Formation by Mycobacterium abscessus in a Lung Cavity. *Am J Respir Crit Care Med* **193**, 692–693 (2016).
- 433 3. E. Tortoli, *et al.*, Emended description of Mycobacterium abscessus, Mycobacterium abscessus subsp. abscessus and Mycobacterium abscessus subsp. bolletii and designation of Mycobacterium abscessus subsp. massiliense comb. nov. *Int J Syst Evol Microbiol* **66**, 4471–4479 (2016).
- 437 4. S. T. Howard, *et al.*, Spontaneous reversion of Mycobacterium abscessus from a
  438 smooth to a rough morphotype is associated with reduced expression of
  439 glycopeptidolipid and reacquisition of an invasive phenotype. *Microbiology (N Y)* **152**,
  440 1581–1590 (2006).
- E. R. Rhoades, *et al.*, Mycobacterium abscessus Glycopeptidolipids Mask Underlying
   Cell Wall Phosphatidyl- myo -Inositol Mannosides Blocking Induction of Human
   Macrophage TNF-α by Preventing Interaction with TLR2. *The Journal of Immunology* 183, 1997–2007 (2009).
- 445 6. R. Nessar, J.-M. Reyrat, L. B. Davidson, T. F. Byrd, Deletion of the mmpL4b gene in 446 the Mycobacterium abscessus glycopeptidolipid biosynthetic pathway results in loss 447 of surface colonization capability, but enhanced ability to replicate in human 448 macrophages and stimulate their innate immune response. *Microbiology (N Y)* **157**, 449 1187–1195 (2011).
- P. Chakraborty, A. Kumar, The extracellular matrix of mycobacterial biofilms: could we shorten the treatment of mycobacterial infections? *Microbial Cell* **6**, 105–122 (2019).
- 452 8. L. Karygianni, Z. Ren, H. Koo, T. Thurnheer, Biofilm Matrixome: Extracellular
  453 Components in Structured Microbial Communities. *Trends Microbiol* **28**, 668–681
  454 (2020).
- P. Vega-Dominguez, *et al.*, Biofilms of the non-tuberculous Mycobacterium chelonae
   form an extracellular matrix and display distinct expression patterns. *The Cell Surface* 100043 (2020).
- 458 10. C. Wiegand, et al., Critical physiological factors influencing the outcome of
   459 antimicrobial testing according to ISO 22196 / JIS Z 2801. PLoS One 13, e0194339
   460 (2018).
- 461 11. J. Azeredo, *et al.*, Critical review on biofilm methods. *Crit Rev Microbiol* **43**, 313–351 (2017).
- 463 12. M. D. Macia, E. Rojo-Molinero, A. Oliver, Antimicrobial susceptibility testing in biofilm-464 growing bacteria. *Clinical Microbiology and Infection* **20**, 981–990 (2014).
- 465 13. K. A. Nash, B. A. Brown-Elliott, R. J. Wallace, A Novel Gene, erm (41), Confers
   466 Inducible Macrolide Resistance to Clinical Isolates of Mycobacterium abscessus but Is
   467 Absent from Mycobacterium chelonae. *Antimicrob Agents Chemother* 53, 1367–1376
   468 (2009).

- 469 14. H.-Y. Kim, *et al.*, Mycobacterium massiliense is differentiated from Mycobacterium
- 470 abscessus and Mycobacterium bolletii by erythromycin ribosome methyltransferase
- gene (erm) and clarithromycin susceptibility patterns. *Microbiol Immunol* **54**, 347–353 (2010).
- 473 15. S. Saxena, H. P. Spaink, G. Forn-Cuní, Drug Resistance in Nontuberculous Mycobacteria: Mechanisms and Models. *Biology (Basel)* **10**, 96 (2021).
- 475 16. K. Andries, *et al.*, A Diarylquinoline Drug Active on the ATP Synthase of Mycobacterium tuberculosis. *Science* (1979) **307**, 223–227 (2005).
- 477 17. A. Koul, *et al.*, Diarylquinolines target subunit c of mycobacterial ATP synthase. *Nat Chem Biol* **3**, 323–324 (2007).
- 479 18. E. Huitric, P. Verhasselt, K. Andries, S. E. Hoffner, In Vitro Antimycobacterial Spectrum 480 of a Diarylquinoline ATP Synthase Inhibitor. *Antimicrob Agents Chemother* **51**, 4202– 4204 (2007).
- 482 19. C. Dupont, *et al.*, Bedaquiline Inhibits the ATP Synthase in Mycobacterium abscessus and Is Effective in Infected Zebrafish. *Antimicrob Agents Chemother* **61** (2017).
- 484 20. Y. Pang, H. Zheng, Y. Tan, Y. Song, Y. Zhao, In Vitro Activity of Bedaquiline against Nontuberculous Mycobacteria in China. *Antimicrob Agents Chemother* **61** (2017).
- 486 21. M. Relucenti, *et al.*, Microscopy Methods for Biofilm Imaging: Focus on SEM and VP-487 SEM Pros and Cons. *Biology (Basel)* **10**, 51 (2021).
- 488 22. L. C. Gomes, F. J. Mergulhão, SEM Analysis of Surface Impact on Biofilm Antibiotic 489 Treatment. *Scanning* **2017**, 1–7 (2017).
- 490 23. L. C. Gomes, L. N. Silva, M. Simões, L. F. Melo, F. J. Mergulhão, Escherichia coli
   491 adhesion, biofilm development and antibiotic susceptibility on biomedical materials. *J* 492 *Biomed Mater Res A* 103, 1414–1423 (2015).
- 493 24. H. Jiang, M. R. Kilburn, J. Decelle, N. Musat, NanoSIMS chemical imaging combined 494 with correlative microscopy for biological sample analysis. *Curr Opin Biotechnol* **41**, 495 130–135 (2016).
- 496 25. P. Santucci, *et al.*, Intracellular localisation of Mycobacterium tuberculosis affects efficacy of the antibiotic pyrazinamide. *Nat Commun* **12**, 3816 (2021).
- 498 26. A. Fearns, D. J. Greenwood, A. Rodgers, H. Jiang, M. G. Gutierrez, Correlative light 499 electron ion microscopy reveals in vivo localisation of bedaquiline in Mycobacterium 500 tuberculosis—infected lungs. *PLoS Biol* **18**, e3000879 (2020).
- 501 27. B. A. Brown-Elliott, R. J. Wallace, In Vitro Susceptibility Testing of Bedaquiline against Mycobacterium abscessus Complex. *Antimicrob Agents Chemother* **63** (2019).
- 503 28. S. Vesenbeckh, *et al.*, Bedaquiline as a potential agent in the treatment of Mycobacterium abscessus infections. *European Respiratory Journal* [Preprint] (2017).
- 505 29. A. Martin, *et al.*, In vitro activity of bedaquiline against slow-growing nontuberculous mycobacteria. *J Med Microbiol* **68**, 1137–1139 (2019).
- 507 30. K. L. Chew, *et al.*, In vitro susceptibility of Mycobacterium abscessus complex and feasibility of standardizing treatment regimens. *J Antimicrob Chemother* **76** (2021).

- M. Lindman, T. Dick, Bedaquiline Eliminates Bactericidal Activity of β-Lactams against
   Mycobacterium abscessus. *Antimicrob Agents Chemother* 63 (2019).
- 511 32. M. M. Ruth, *et al.*, A bedaquiline/clofazimine combination regimen might add activity to the treatment of clinically relevant non-tuberculous mycobacteria. *Journal of Antimicrobial Chemotherapy* **74**, 935–943 (2019).
- 514 33. L. Thieme, *et al.*, MBEC Versus MBIC: the Lack of Differentiation between Biofilm Reducing and Inhibitory Effects as a Current Problem in Biofilm Methodology. *Biol Proced Online* **21**, 18 (2019).
- 517 34. G. Clary, *et al.*, Mycobacterium abscessus Smooth and Rough Morphotypes Form 518 Antimicrobial-Tolerant Biofilm Phenotypes but Are Killed by Acetic Acid. *Antimicrob* 519 *Agents Chemother* **62** (2018).
- 520 35. Y. K. Yam, N. Alvarez, M. L. Go, T. Dick, Extreme Drug Tolerance of Mycobacterium abscessus "Persisters." *Front Microbiol* **11** (2020).
- 522 36. M.-C. Muñoz-Egea, M. García-Pedrazuela, I. Mahillo, J. Esteban, Effect of 523 ciprofloxacin in the ultrastructure and development of biofilms formed by rapidly 524 growing mycobacteria. *BMC Microbiol* **15**, 18 (2015).
- 525 37. Y. Okae, *et al.*, Estimation of Minimum Biofilm Eradication Concentration (MBEC) on In Vivo Biofilm on Orthopedic Implants in a Rodent Femoral Infection Model. *Front Cell Infect Microbiol* **12** (2022).
- 528 38. P. Castaneda, A. McLaren, G. Tavaziva, D. Overstreet, Biofilm Antimicrobial 529 Susceptibility Increases With Antimicrobial Exposure Time. *Clin Orthop Relat Res* 530 **474**, 1659–1664 (2016).
- 39. J. Esteban, M. García-Coca, Mycobacterium Biofilms. Front Microbiol 8 (2018).
- 532 40. E. I. Niño-Padilla, C. Velazquez, A. Garibay-Escobar, Mycobacterial biofilms as players in human infections: a review. *Biofouling* **37** (2021).
- 534 41. T. Tran, A. J. Bonham, E. D. Chan, J. R. Honda, A paucity of knowledge regarding nontuberculous mycobacterial lipids compared to the tubercle bacillus. *Tuberculosis* 115, 96–107 (2019).
- 537 42. S. T. Howard, *et al.*, Spontaneous reversion of Mycobacterium abscessus from a smooth to a rough morphotype is associated with reduced expression of glycopeptidolipid and reacquisition of an invasive phenotype. *Microbiology (N Y)* **152**, 1581–1590 (2006).
- K. Rüger, et al., Characterization of Rough and Smooth Morphotypes of
   Mycobacterium abscessus Isolates from Clinical Specimens. J Clin Microbiol 52, 244–
   250 (2014).
- 544 44. R. Greendyke, T. F. Byrd, Differential antibiotic susceptibility of Mycobacterium abscessus variants in biofilms and macrophages compared to that of planktonic bacteria. *Antimicrob Agents Chemother* **52** (2008).
- 547 45. A. Bernut, *et al.*, Insights into the smooth-to-rough transitioning in Mycobacterium 548 bolletii unravels a functional Tyr residue conserved in all mycobacterial MmpL family 549 members. *Mol Microbiol* **99**, 866–883 (2016).
- 550 46. J. Esteban, M. García-Coca, Mycobacterium Biofilms. Front Microbiol 8 (2018).

- 551 47. M. M. Williams, et al., Structural Analysis of Biofilm Formation by Rapidly and Slowly
- Growing Nontuberculous Mycobacteria. *Appl Environ Microbiol* **75**, 2091–2098
- 553 (2009).

586

587

588

- 554 48. A. Dokic, *et al.*, Mycobacterium abscessus biofilms produce an extracellular matrix and have a distinct mycolic acid profile. *The Cell Surface* **7**, 100051 (2021).
- 556 49. L. Karygianni, Z. Ren, H. Koo, T. Thurnheer, Biofilm Matrixome: Extracellular
- 557 Components in Structured Microbial Communities. *Trends Microbiol* **28**, 668–681 (2020).
- 559 50. P. Chakraborty, A. Kumar, The extracellular matrix of mycobacterial biofilms: could we shorten the treatment of mycobacterial infections? *Microbial Cell* **6**, 105–122 (2019).
- 561 51. A. V. Gutiérrez, A. Viljoen, E. Ghigo, J.-L. Herrmann, L. Kremer, Glycopeptidolipids, a Double-Edged Sword of the Mycobacterium abscessus Complex. *Front Microbiol* **9** (2018).
- 564 52. P. López-Roa, J. Esteban, M.-C. Muñoz-Egea, Updated Review on the Mechanisms of Pathogenicity in Mycobacterium abscessus, a Rapidly Growing Emerging Pathogen. *Microorganisms* **11**, 90 (2022).
- 567 53. N. Kwak, *et al.*, Mycobacterium abscessus pulmonary disease: Individual patient data meta-analysis. *European Respiratory Journal* **54** (2019).
- 54. W. J. Koh, J. E. Stout, W. W. Yew, Advances in the management of pulmonary
   disease due to Mycobacterium abscessus complex. *International Journal of Tuberculosis and Lung Disease* [Preprint] (2014).
- 572 55. P. H. C. Candido, *et al.*, Multidrug-resistant nontuberculous mycobacteria isolated from cystic fibrosis patients. *J Clin Microbiol* **52** (2014).
- 574 56. E. S. Gloag, D. J. Wozniak, P. Stoodley, L. Hall-Stoodley, Mycobacterium abscessus 575 biofilms have viscoelastic properties which may contribute to their recalcitrance in 576 chronic pulmonary infections. *Sci Rep* **11** (2021).
- 577 57. P. J. Brennan, H. Nikaido, The Envelope of Mycobacteria. *Annu Rev Biochem* **64** (1995).
- 579 58. K. Laurent, G. S. Besra, "A Waxy Tale, by Mycobacterium tuberculosis" in *Tuberculosis and the Tubercle Bacillus*, (2014).
- 581 59. E. Gil, *et al.*, Bedaquiline as treatment for disseminated nontuberculous mycobacteria infection in 2 patients co-infected with HIV. *Emerg Infect Dis* **27** (2021).
- G. McMahon, C. P. Lechene, High-Resolution Multi-Isotope Imaging Mass
   Spectrometry (MIMS) Imaging Applications in Stem Cell Biology. *Curr Protoc* 1 (2021).

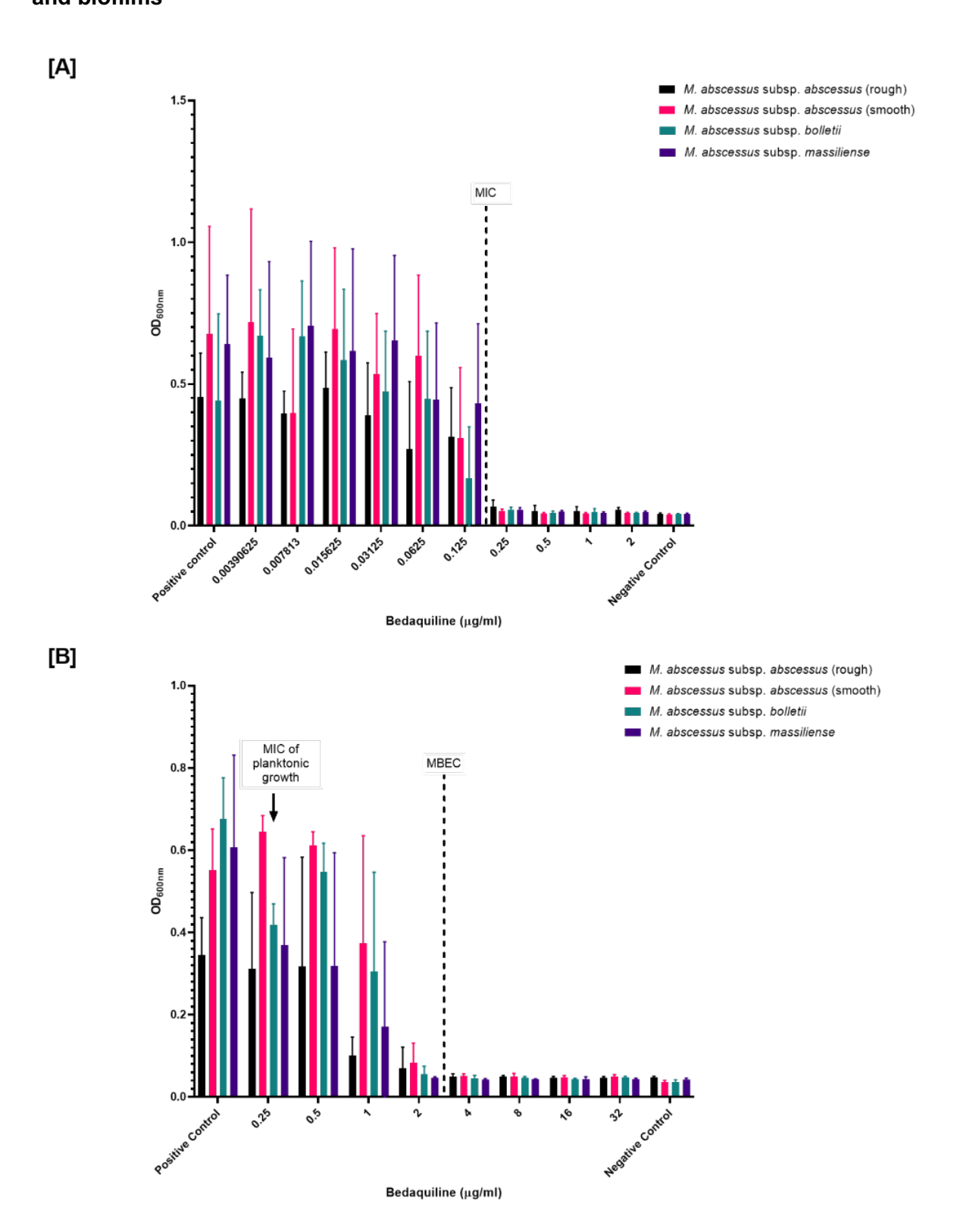
# **Figures and Tables**

590

591

592

# Figure 1: Determining the efficacy of Bedaquiline against MABC in planktonic growth and biofilms



[A] Antibiotic concentrations of BDQ were conducted in two-fold serial dilutions in a 96 well plate to determine the MIC. The OD $_{600nm}$  in each well of the microtiter plate was measured after incubation at 37°C. The MIC was taken as the lowest concentration that inhibited MABC growth. The MIC for MABC was 0.25  $\mu$ g/ml. [B] Using the MIC of the MABC as an initial concentration, the MBEC for BDQ against MABC biofilms were determined. Mature biofilms formed on the pegs of the device, were exposed to a two-fold serially diluted BDQ in a 96 well plate to determine the MBEC. After incubation for 24 hours at 37°C, the OD $_{600nm}$  in each well of the microtiter plate was measured. The MBEC of MABC biofilms was 4  $\mu$ g/ml. Results were expressed as the mean  $\pm$  standard deviation (SD) of three independent experiments.

# Table 1: The MBC, MBIC, MBEC and BBC of BDQ against MABC biofilms using MBEC

# assay

628629

630

631

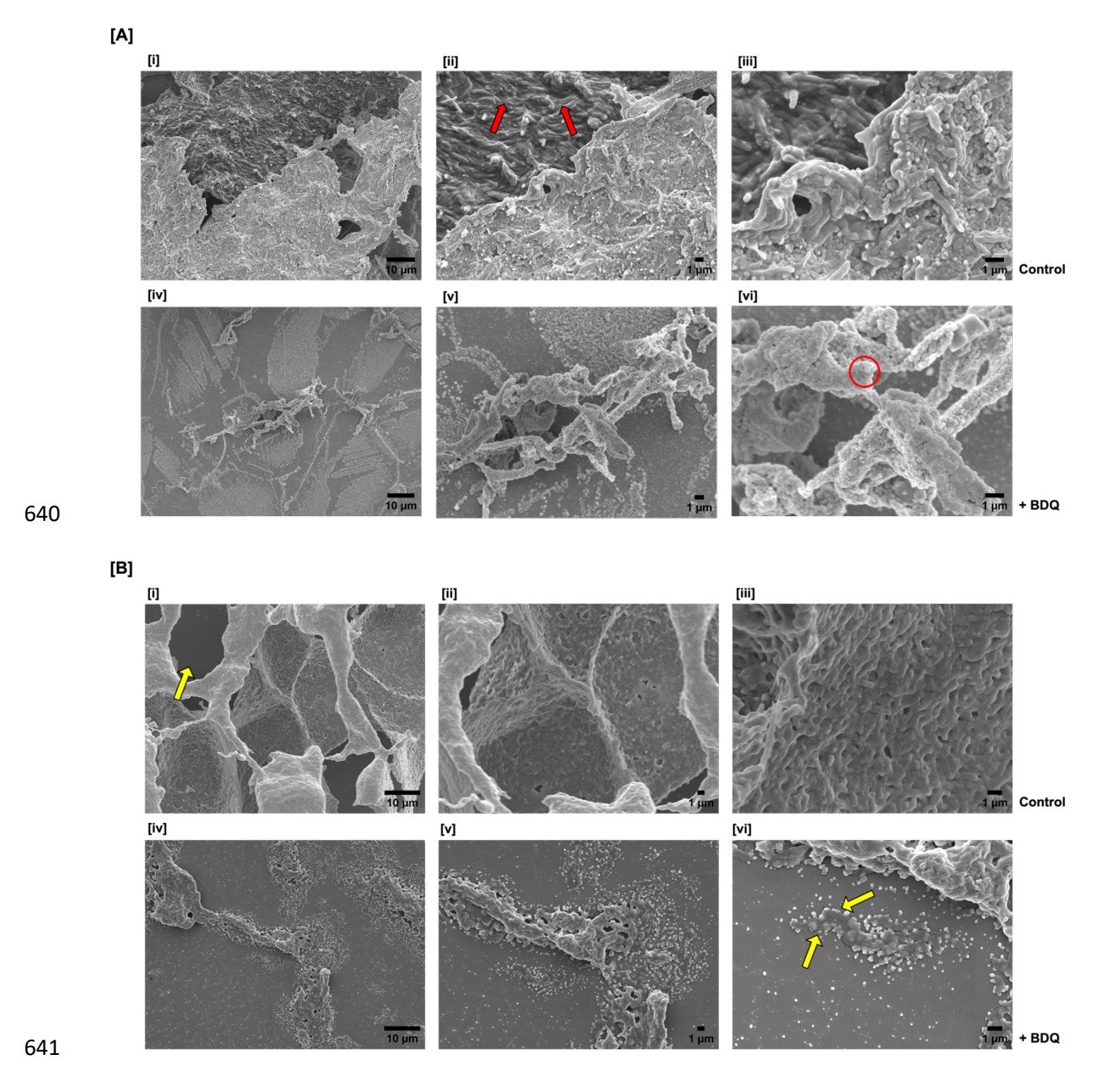
	BDQ (μg/ml)			
	MBC <sup>1</sup>	MBIC <sup>2</sup>	MBEC <sup>3</sup>	BBC <sup>4</sup>
M. abscessus subsp. abscessus (rough)	4	4	4	>32
M. abscessus subsp. abscessus (smooth)	4	4	4	>32
M. abscessus subsp. bolletii	4	16	4	>32
M. abscessus subsp. massiliense	2	1	2	32

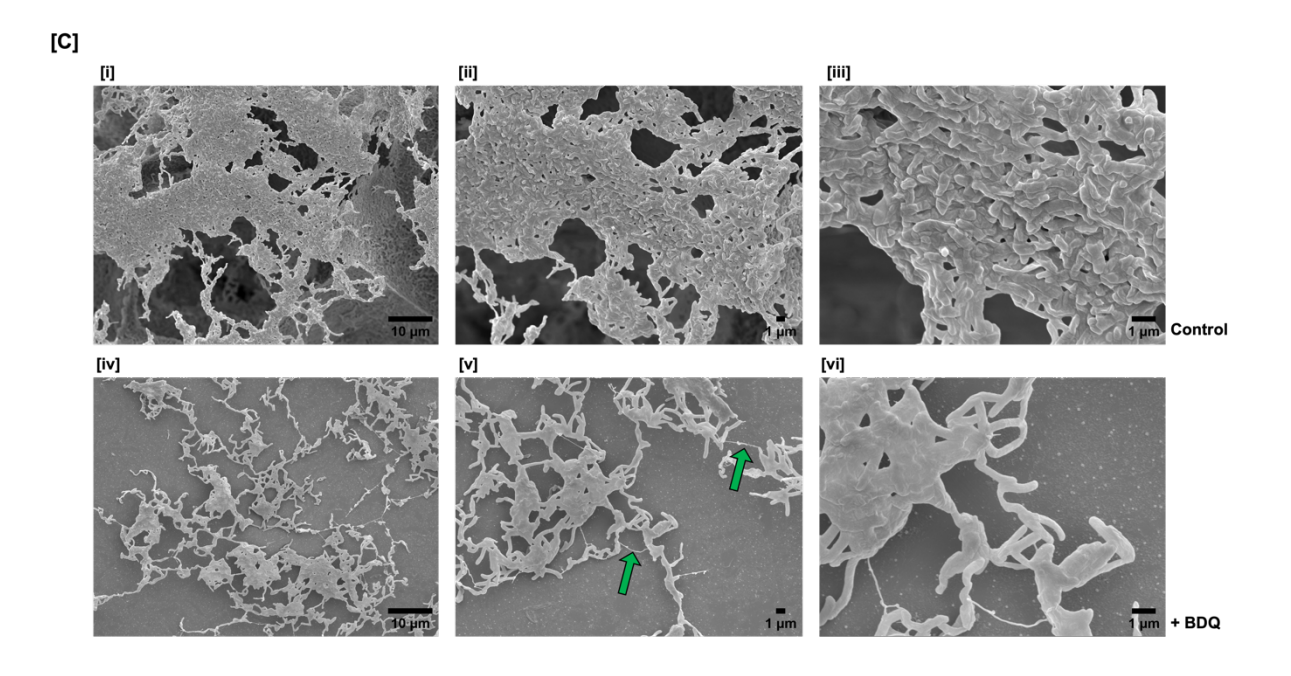
<sup>&</sup>lt;sup>1</sup>MBC = minimal bactericidal concentration; <sup>2</sup>MBIC = minimal biofilm inhibitory concentration;

<sup>&</sup>lt;sup>3</sup>MBEC = minimal biofilm eradication concentration; <sup>4</sup>BBC = biofilm bactericidal concentration

# Figure 2: SEM analysis of MABC biofilms with and without BDQ

SEM micrographs illustrating the effects BDQ had on MABC biofilms. [(i-iii), increasing magnification] MABC biofilms without antibiotic showed bacilli embedded within an extracellular matrix (ECM). [(iv-vi), increasing magnification] After exposure to BDQ for 24 hours, MABC biofilms showed morphological changes within the structure. [A] *M. abscessus* subsp. *abscessus* (Rough) [B] *M. abscessus* subsp. *abscessus* (Smooth) [C] *M. abscessus* subsp. *bolletii* [D] *M. abscessus* subsp. *massiliense*.





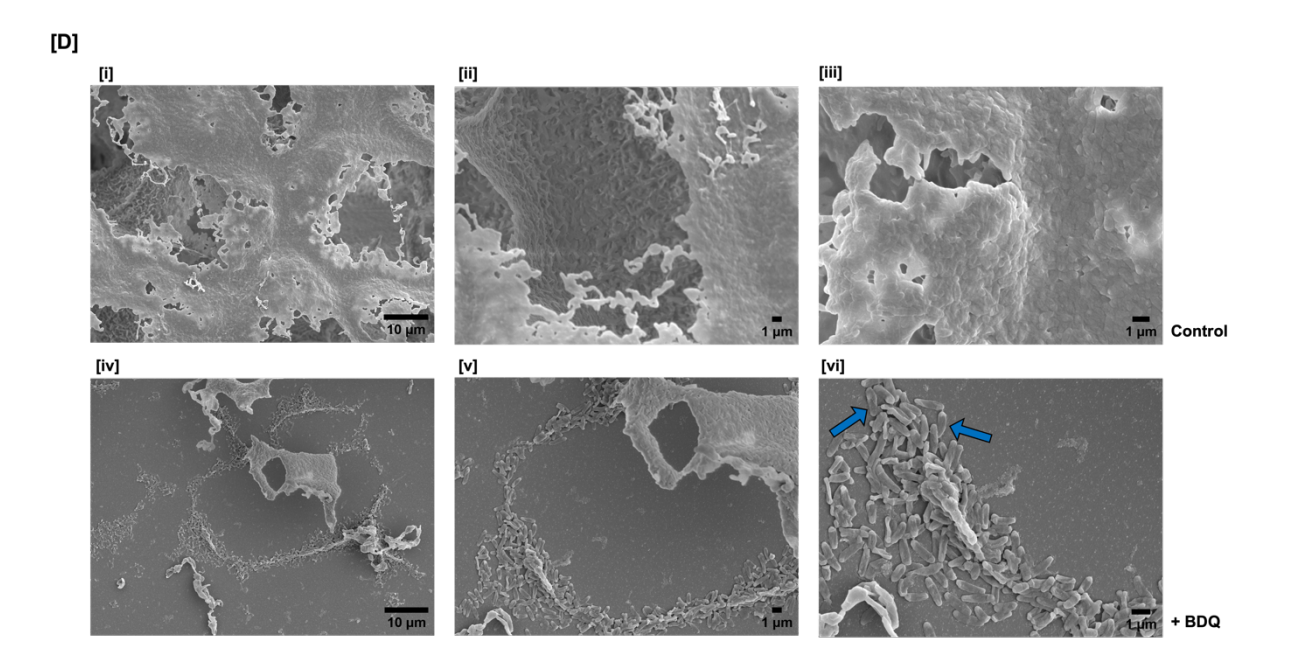
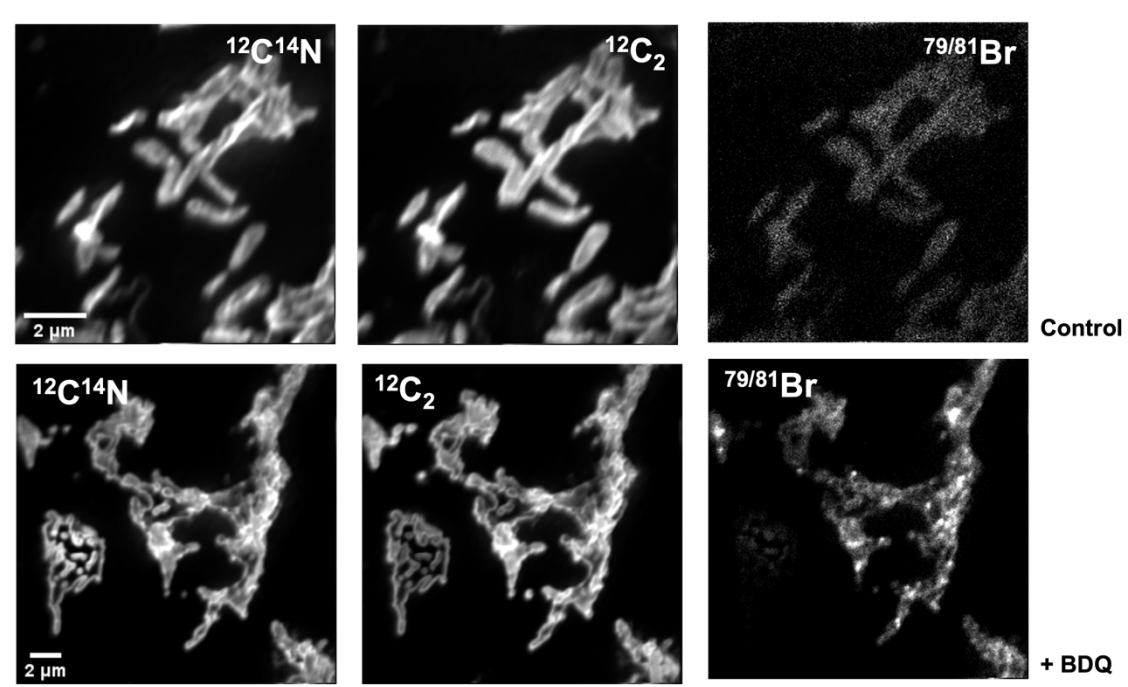
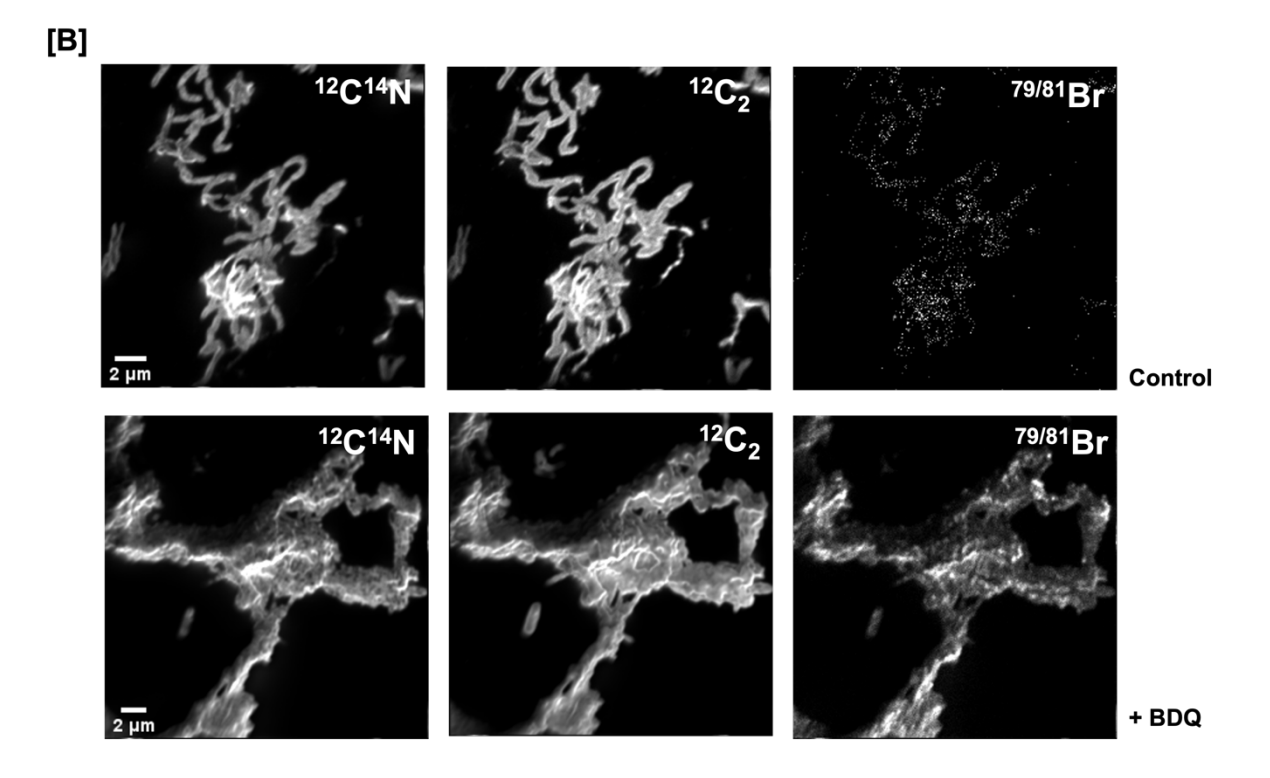


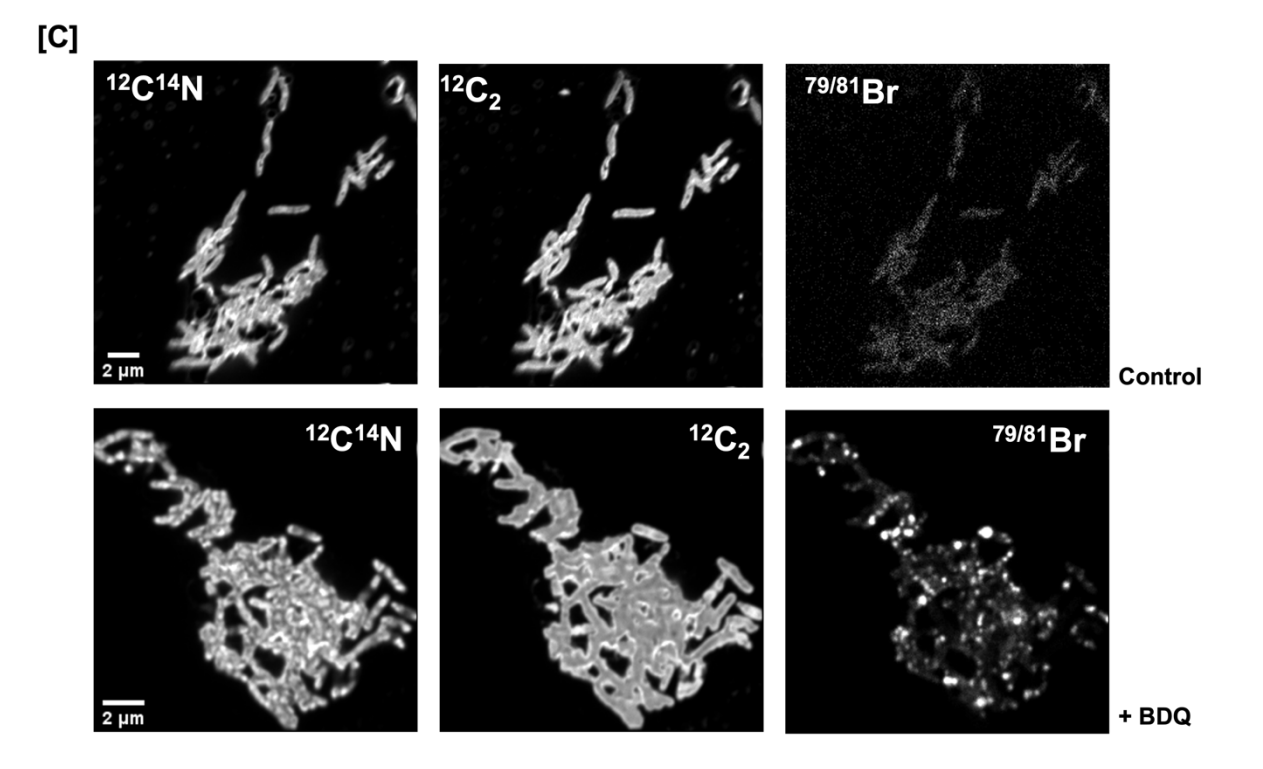
Figure 3: NanoSIMS micrographs of MABC biofilms treated with and without BDQ

Secondary ion images of cellular components of the biofilm ( $^{12}C^{14}N^-$  and  $^{12}C_2^-$ ) and BDQ (Br). Control MABC biofilms (Top Row) and MABC biofilms treated with BDQ for 24hrs (Bottom Row). **[A]** *M. abscessus* subsp. *abscessus* (Rough) **[B]** *M. abscessus* subsp. *abscessus* subsp. *massiliense*. Images are representative of randomly selected regions from three biological samples and three technical repeats.









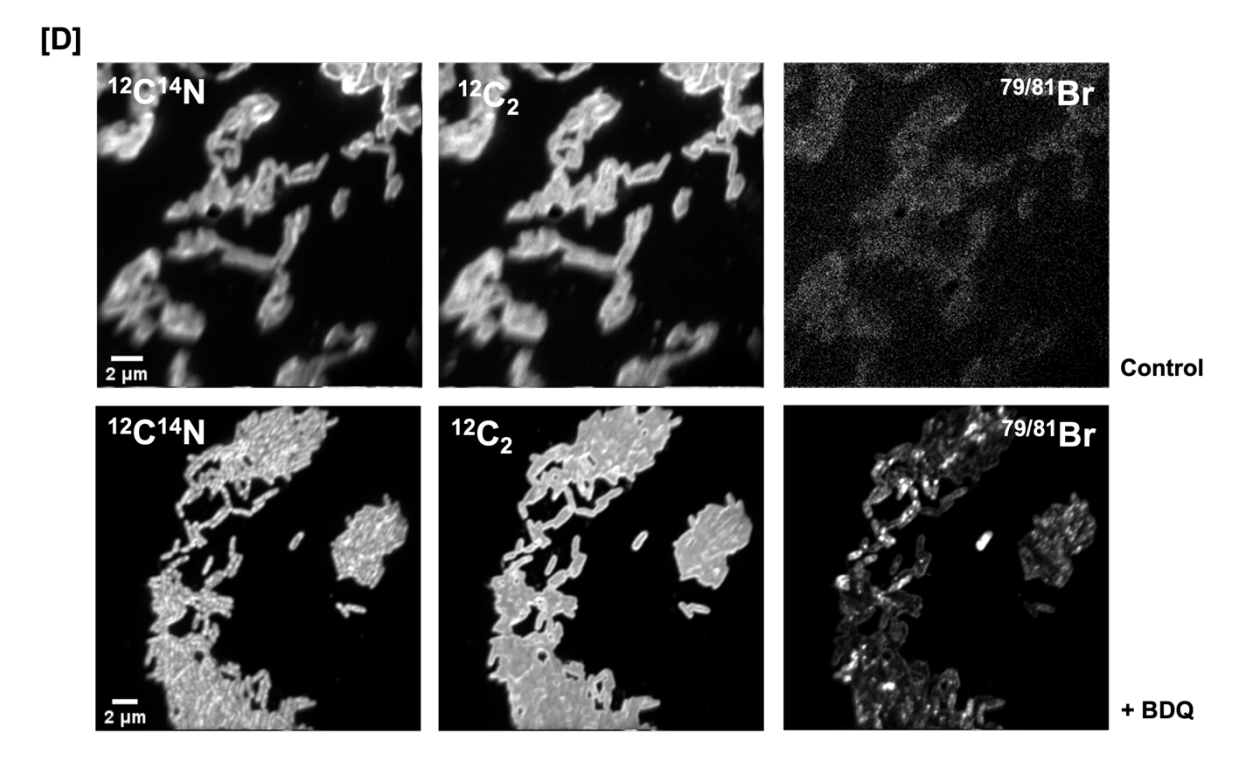


# Figure 4: Quantitative analysis of BDQ distribution within the cellular components of MABC biofilms

Quantitative analysis using ratio distribution **[A]** Br $^{-1/2}C^{14}N^{-1}$  **[B]** Br $^{-1/2}C_{2}^{-1}$  of MABC biofilms with and without BDQ. Results were obtained from 32-61 individually segmented bacteria (from three biological samples and three technical repeats) and the p-values were calculated by using a Two-Way Anova. Pair-wise significant differences indicated by different letters.

